Nucleon Spin Structure and Parton Distribution Functions

Jörg Pretz[1] on behalf of the *COMPASS* Collaboration
Physikalisches Institut
Universität Bonn
D-53115 Bonn, GERMANY

This article gives an overview over recent results on quark and gluon helicity distributions obtained in deep inelastic lepton nucleon scattering and proton proton interactions. Future experimental programs to study the nucleon structure will be discussed as well.

1 Introduction

In the Quark Parton Model, the nucleon is successfully described in terms of parton distribution functions (PDFs). Whereas unpolarized parton distributions like $q(x)$ and $g(x)$ interpreted as number densities of quarks and gluons at a given longitudinal momentum fraction x in the nucleon are relatively well known, distributions involving polarization degrees of freedom are less well known. The most prominent ones, related to the nucleon spin problem, are the helicity distributions $\Delta q(x)$, $\Delta g(x)$ and the transversity distributions $\Delta q_T(x)$.

This paper focuses on the helicity distributions. Effects occurring when considering transverse momenta and transverse polarizations are discussed in the contribution of M. Anselmino [3]. Section 2 gives a short summary of the nucleon spin puzzle and its connection to helicity distributions of quarks and gluons. Section 3 discusses various experimental methods to access the helicity distributions. Recent results are presented in Section 4. Future experimental programs are discussed in Section 5.

2 The nucleon spin puzzle

The spin of the nucleon can be decomposed in helicity ($\Delta\Sigma$ & ΔG) and orbital angular momentum contributions (L_q & L_g) of quarks and gluons

$$\frac{1}{2} = \frac{1}{2}\Delta\Sigma + \Delta G + L_q + L_g \ .$$

[1]jorg.pretz@cern.ch

For a recent discussion on ambiguities in this decomposition see [1]. Whereas the static quark model predicts $\Delta\Sigma = 1$ and zero contribution from ΔG, L_q and L_g, relativistic quark models predict a helicity contribution of quarks, $\Delta\Sigma$ of the order of 60% [2]. Results from polarized deep inelastic scattering indicate a much smaller value: $\Delta\Sigma \approx 25\%$, allowing thus for large contributions of ΔG, L_q and L_g. In recent years mainly the measurement of ΔG was in the focus of research because a large contribution $\Delta G \approx 2-3$ could explain the small value of $\Delta\Sigma$ measured in deep inelastic scattering via the mechanism of axial anomaly [4]. While a contribution of 400 – 600 % (corresponding to $\Delta G = 2-3$) of the gluon helicity to the nucleon spin may sound strange, one should keep in mind that although perturbative QCD is not able to predict ΔG, it can predict its scale dependence. It is given by $\Delta G(\mu)\alpha_s(\mu) = \text{const.}$ in next-to-leading order (NLO) QCD, i.e. with increasing scale μ, ΔG must increase because the strong coupling constant α_s decreases.

The helicity contributions of quarks, $\Delta\Sigma$ can be further decomposed in the contributions of different quark flavors depending on the momentum fraction x carried by the quarks:

$$\Delta\Sigma = \int_0^1 \sum_q \Delta q(x)\mathrm{dx}$$

where the sum runs over all light quark flavors $q = u, d, s, \overline{u}, \overline{d}, \overline{s}$. The helicity distribution is defined as $\Delta q(x) = q^{\uparrow}(x) - q^{\downarrow}(x)$, the unpolarized distributions are given by $q(x) = q^{\uparrow}(x) + q^{\downarrow}(x)$. Similar to the unpolarized quark distributions $q^{\uparrow}(x)(q^{\downarrow}(x))$ are number densities of quarks with spin parallel (anti-parallel) to the nucleon spin.

In a similar way the first moment of the gluon distribution is given by the integral over the gluon helicity distribution

$$\Delta G = \int_0^1 \Delta g(x)\mathrm{d}x\,.$$

As mentioned above, presently we know that $\Delta\Sigma$ is of the order of 25%. Open questions addressed in this article are the distribution of these 25% among the different quark flavors and new results on the gluon helicity distribution $\Delta g(x)$.

3 Accessing the helicity distributions

Helicity distributions can be accessed in deep inelastic scattering and proton-proton scattering. The most simple case of inclusive polarized deep inelastic scattering

$$\vec{\ell} + \vec{N} \rightarrow \ell' + X$$

will be discussed in more detail. In all reactions mentioned X stands for unobserved final state particles. A polarized lepton creates a polarized photon. By changing the relative spin orientation of lepton and nucleon the two situations shown in Fig. 1 are obtained. In the

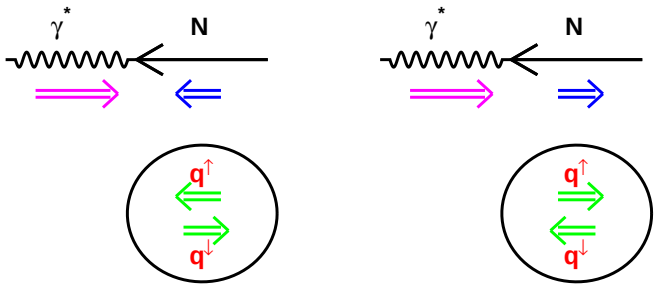

Figure 1: Accessing the helicity distributions in polarized deep inelastic scattering. Double arrows indicate the spin direction.

left diagram photon and nucleon spins are antiparallel. In this case the photon can only be absorbed by a quark having its spin aligned with the nucleon spin ($q^{\uparrow}$). The absorption of the photon by the quark having its spin anti-aligned with the nucleon spin would result in quark with $J_z = 3/2$ in the final state and is thus forbidden. In a similar way, if photon and nucleon spin are aligned (Fig. 1, right) the photon can only be absorbed by a quark having its spin anti-aligned with the nucleon spin ($q^{\downarrow}$).

The photon-nucleon cross section asymmetry denoted by A_1 is thus given by

$$A_1(x) = \frac{\sigma^{\uparrow\downarrow}_{\gamma^* N} - \sigma^{\uparrow\uparrow}_{\gamma^* N}}{\sigma^{\uparrow\downarrow}_{\gamma^* N} + \sigma^{\uparrow\uparrow}_{\gamma^* N}} = \frac{\sum_q e_q^2(\Delta q(x) + \Delta\bar{q}(x))}{\sum_q e_q^2(q(x) + \bar{q}(x))}, \tag{1}$$

e_q being electric charge of the quark $q = u, d, s$.

Selecting specific hadronic final states, h, in semi-inclusive deep inelastic scattering

$$\vec{\ell} + \vec{N} \to \ell' + h + X$$

allows to get more detailed information on the quark helicity distributions. The corresponding photon-nucleon asymmetry reads

$$A_1^h(x,z) = \frac{\sum_q e_q^2 \left(\Delta q(x) D_q^h(z) + \Delta\bar{q}(x) D_{\bar{q}}^h(z)\right)}{\sum_q e_q^2 \left(q(x) D_q^h(z) + \bar{q}(x) D_{\bar{q}}^h(z)\right)}. \tag{2}$$

The fragmentation functions $D_q^h(z)$ describe the probability that a quark q fragments into a hadron h carrying an energy fraction z of the virtual photon energy ν in the target rest frame. Semi-inclusive deep inelastic scattering allows to separate contributions from quarks and anti-quarks because in general the corresponding fragmentation functions differ ($D_q^h \neq D_{\bar{q}}^h$). Moreover, by selecting strange hadrons (K^+ and K^-) one can for example enhance the contribution of the strange quarks.

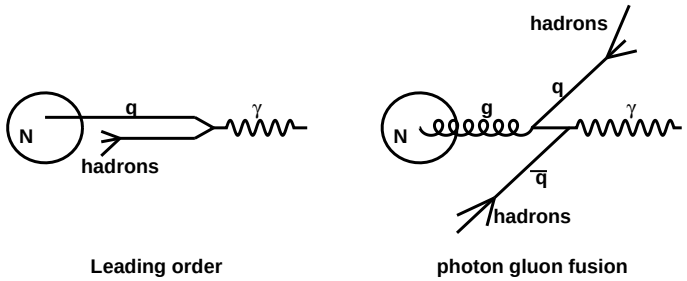

Figure 2: Leading Order (LO) and photon-gluon-fusion (PGF) process in deep inelastic scattering.

Another possibility to measure the quark helicity distributions is polarized pp scattering. Single spin asymmetries of the process

$$\vec{p} + p \to W^{\pm} + \cdots \to e^{\pm} + \ldots$$

give access to quark helicity distributions with the advantage that no knowledge on fragmentation functions is needed. These single spin asymmetries are related to the helicity distributions in the following way

$$A_L^{W^+} = \frac{\Delta\overline{d}(x_1)u(x_2) - \Delta u(x_1)\overline{d}(x_2)}{u(x_1)\overline{d}(x_2) + \overline{d}(x_1)u(x_2)}, \quad A_L^{W^-} = \frac{\Delta\overline{u}(x_1)d(x_2) - \Delta d(x_1)\overline{u}(x_2)}{d(x_1)\overline{u}(x_2) + \overline{u}(x_1)d(x_2)}.$$

Accessing the gluon helicity distribution is more difficult. It can for example be done by a next-to-leading order (NLO) analysis of spin asymmetries where the leading order (LO) expression given in Eqs. (1) and (2) are modified and receive contributions involving $\Delta g(x)$. Another possibility is to look for hadronic final states tagging the participation of gluons in the scattering process. This can be done by selecting for example hadrons with large transverse momentum with respect to the virtual photon axis or charmed mesons. This is illustrated in Fig. 2. In a leading order process where the photon is absorbed by one of the quarks, hadrons are essentially produced along the axis of the virtual photon (Fig. 2 left). If a gluon participates in the partonic sub-process, hadrons can be produced at larger p_T (Fig. 2 right). A particular clean tag of the gluon in the partonic subprocess is the detection of a charmed meson D^0 or D^* in the final state, because these are almost exclusively produced via the process $\gamma + g \to c + \bar{c}$.

In polarized pp scattering double spin asymmetries for various final states gives access to gluon helicity contribution. These asymmetries depend on the product of parton helicity distributions Δq^2, Δg^2 and $\Delta q \times \Delta g$.

4 Results

4.1 Quark Helicity distributions

Figure 3 shows the inclusive asymmetry A_1^p obtained from several experiments in deep inelastic scattering of polarized electrons or muons on polarized protons vs. the Bjorken variable x, which equals in LO the parton momentum fraction, for a momentum transfer $Q^2 > 1\text{GeV}^2$. Note that due to the different center of mass energies data points at a given x may have different values of Q^2.

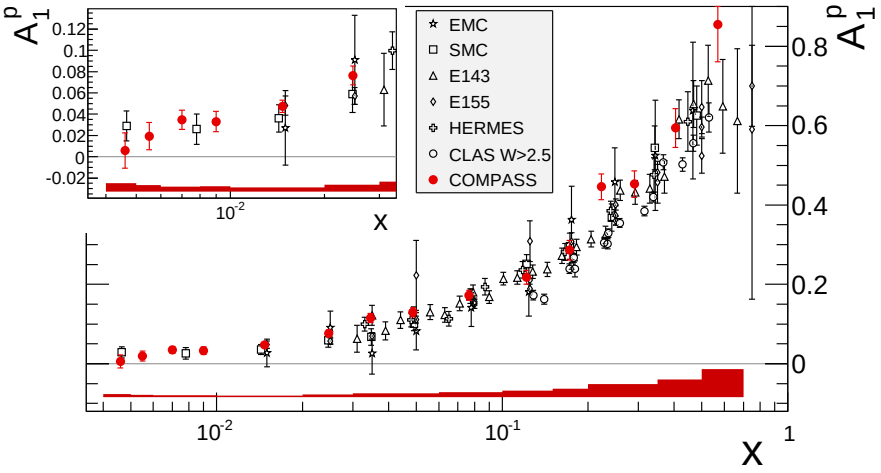

Figure 3: Results for the inclusive asymmetry A_1^p [5].

Using these asymmetries together with the corresponding asymmetries for neutron and deuteron and information from the neutron and hyperon decay constants results in the values for the first moments of the quark distributions given in Table 1. The most right column shows results from Lattice QCD calculations which are in remarkable agreement with the results obtained from experiment.

As discussed in Section 3 inclusive deep inelastic scattering gives only access to the sum quark and anti-quark contributions because $e_q^2 = e_{\bar{q}}^2$, whereas semi-inclusive deep inelastic scattering allows to separate contribution from quarks and anti-quarks. Figure 4 shows semi-inclusive asymmetries measured on a proton target together with the inclusive asymmetry from the COMPASS and HERMES experiment.

From these asymmetries together with asymmetries measured on the deuteron target the quark helicity distributions are determined. The analysis is done in leading order QCD where the measured asymmetries are related to the helicity distribution via the following

Table 1: First moments of the polarized quark distributions at $Q^2 = 10\text{GeV}^2$. Note that the error for the result on the global analysis does not include an uncertainty for the unmeasured region 0<x<0.001.

		global analysis [6]	lattice QCD [8]
$\Delta\Sigma$	=	0.25 ± 0.05	
$\Delta u + \Delta\overline{u}$	=	0.81 ± 0.03	0.82 ± 0.04
$\Delta d + \Delta\overline{d}$	=	-0.46 ± 0.03	-0.41 ± 0.04
$\Delta s + \Delta\overline{s}$	=	-0.11 ± 0.06	

matrix equation:

$$\begin{aligned} \vec{A}(x) &= B\left(q(x), \int D_q^h(z)\mathrm{d}z\right)\Delta\vec{q}(x) \quad \text{with} \\ \vec{A} &= (A_{1,p}, A_{1,p}^{\pi^+}, A_{1,p}^{\pi^-}, A_{1,p}^{K^+}, A_{1,p}^{K^-}, A_{1,d}, A_{1,d}^{\pi^+}, A_{1,d}^{\pi^-}, A_{1,d}^{K^+}, A_{1,d}^{K^-}) \\ \Delta\vec{q} &= (\Delta u, \Delta d, \Delta s, \Delta\overline{u}, \Delta\overline{d}, \Delta\overline{s}) \end{aligned} \tag{3}$$

The matrix B connecting the asymmetries with the helicity distributions depends on the unpolarized quark distributions and the fragmentation functions. Systematic errors originating form the choice of fragmentation functions are discussed in the contribution of N. Makke [9].

Figure 5 shows the results assuming $\Delta s = \Delta\overline{s}$ published in Ref. [10]. Dropping this assumption, no difference was observed between Δs and $\Delta\overline{s}$. It only led to an increase in statistical error for the other helicity distributions. Δu is positive and Δd is negative mainly at large x. The sea quark distributions are all close to zero over the whole measured range $0.004 < x < 0.3$. For the strange quark one finds $\int_{0.004}^{0.3} \Delta s(x)\mathrm{d}x = -0.01 \pm 0.01 \pm 0.01$. The large negative value in Table. 1 comes mainly from the unmeasured low x region and is constrained from the neutron and hyperon decay constants. The truncated first moment $\int_{0.004}^{0.3} \Delta\overline{u}(x) - \Delta\overline{d}(x)\mathrm{d}x = 0.06 \pm 0.04(\text{stat}) \pm 0.02(\text{syst})$ is slightly positive and disfavors models with $\Delta\overline{u}(x) - \Delta\overline{d}(x) < 0$.

First results on single spin asymmetries via the exchange of a $W^\pm$ measured by the PHENIX and STAR collaborations at $\sqrt{s} = 500$ GeV at RHIC/BNL are shown in Fig. 6. The measured asymmetries have the expected sign, as can be seen by comparing them to the curves in the Figure which result from various global analyses. To compete with the results from deep inelastic scattering more data are needed.

4.2 Gluon helicity distribution

Figure 7 (left) shows the result on $\Delta g/g$ from direct measurements from deep inelastic scattering using double spin asymmetries of high p_T hadrons and open charm production.

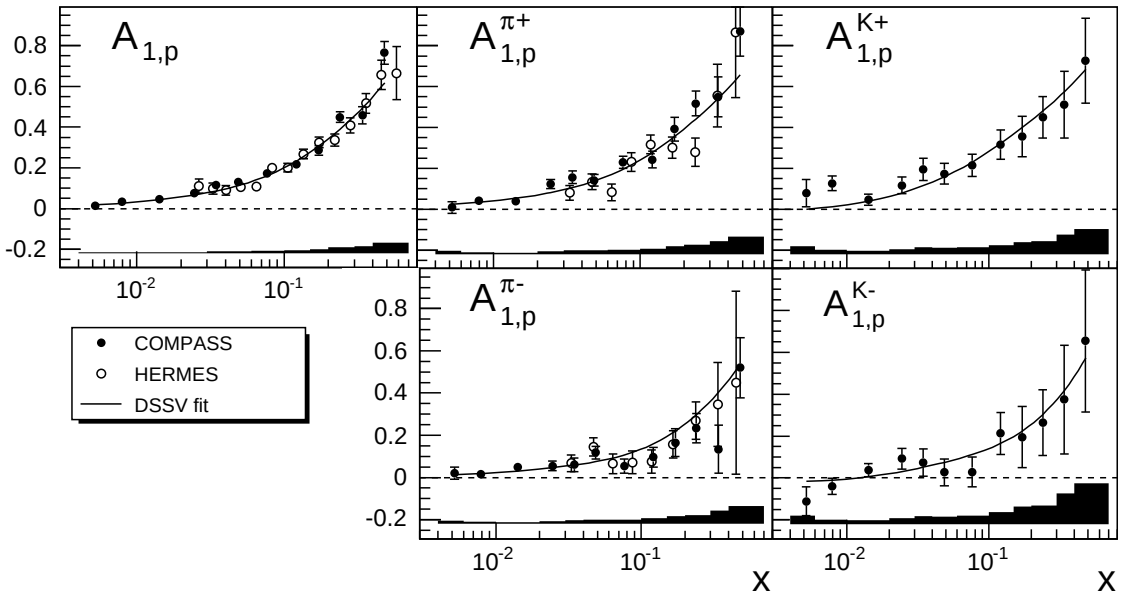

Figure 4: The inclusive and semi-inclusive asymmetry for π^+, π^-, K^+ and K^- for the proton target vs. x from the COMPASS and the HERMES experiment.

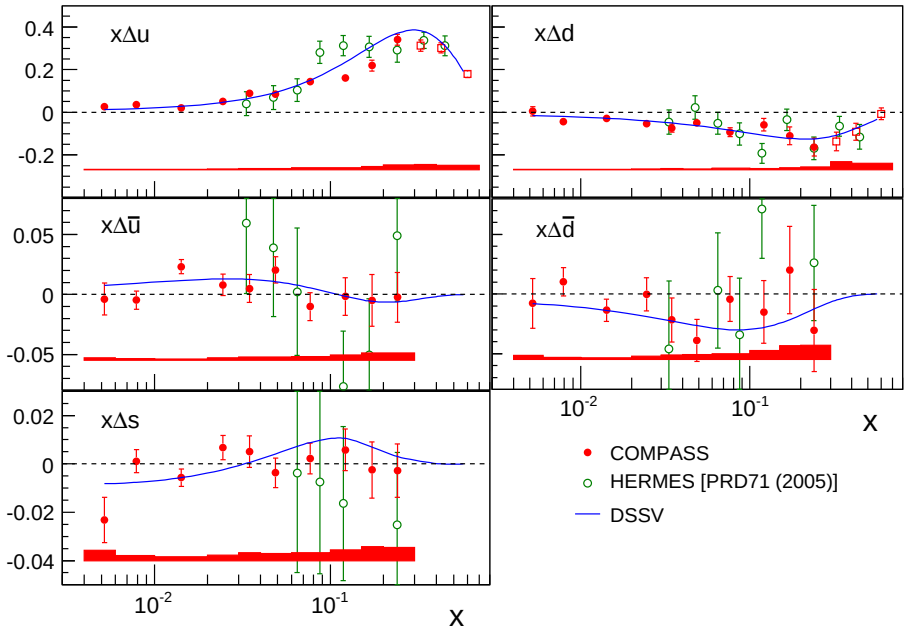

Figure 5: The quark helicity distributions determined from inclusive and semi-inclusive asymmetries.

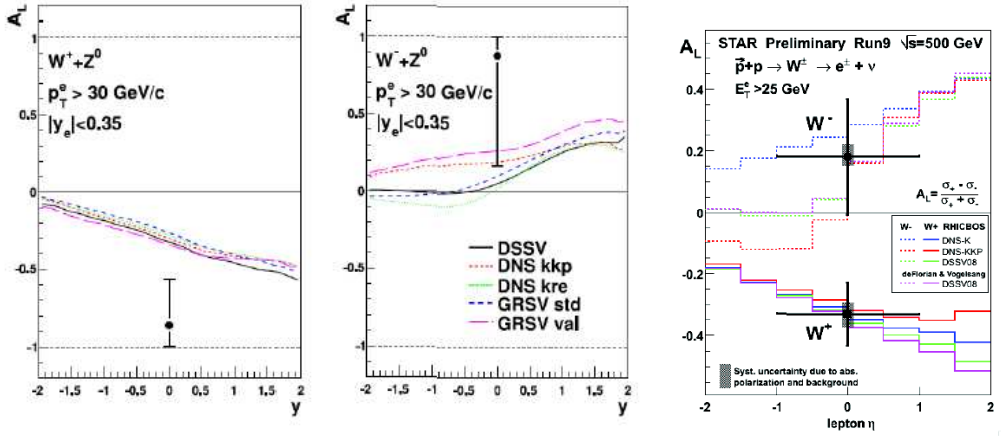

Figure 6: The single spin asymmetry $A_L^{W^+}$ (left) and $A_L^{W^-}$ (right) from the PHENIX [11] experiment and the $A_L^{W^\pm}$ (right) from the STAR [12] experiment as a function of the lepton rapidity compared to results from global analyses of deep inelastic scattering data.

The measured asymmetries are directly related to the polarizations of gluons $\Delta g/g$:

$$A \propto \frac{\Delta g}{g} + A_{\text{bgd}} \cdot$$

All results indicate that $\Delta g/g$ is small in the measured region $x_g \approx 0.1$ certainly excluding large values $\Delta G = 2 - 3$. Here the data where analyzed in LO QCD [2]. For the open charm data also a NLO analysis is available. The result is shown in Fig. 7 (right) together with results of various global analyses. Note that the vertical error bars indicate statistical and systematic error, whereas the horizontal error bars indicate the x_g range covered by the data.

Double spin asymmetries in pp scattering from π^0 production (PHENIX) and jet production (STAR) are shown in Fig. 8. Comparing these asymmetries measured as a function of the transverse momentum p_T with parameterizations gives information on $\Delta g(x)$. More results on $\Delta g(x)$ from the pp scattering at the RHIC experiments are discussed in the contribution of E. Aschenauer [7].

Results from a global NLO QCD analysis including inclusive, semi-inclusive asymmetries as well as asymmetries from pp scattering are shown in Fig. 9 [6]. Note that the newest COMPASS semi-inclusive results and most recent RHIC results are not yet included in this analysis, but they will not change the overall picture [14].

The results on $\Delta u + \Delta\overline{u}$ and $\Delta d + \Delta\overline{d}$ are driven by the inclusive asymmetries, whereas the sea quark contributions are mainly determined by the semi-inclusive asymmetries. The

[2] The LO process in this context is the lowest order diagram involving a gluon, thus the PGF-diagram shown in Fig. 2 (right)

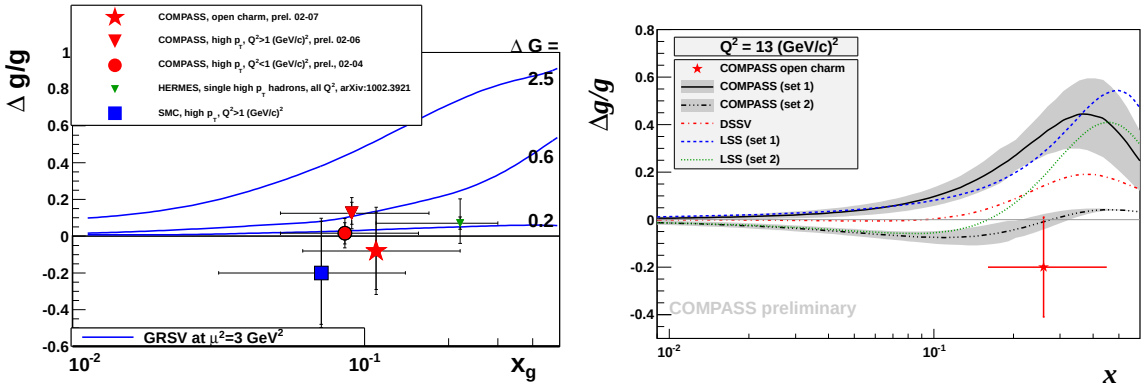

Figure 7: Left: Results from direct measurements of $\Delta g/g$ using a LO QCD analysis. The three blue lines are parameterization corresponding to three different first moments of ΔG.
Right: NLO result from the COMPASS open charm data together with three analyses: COMPASS: global analysis of inclusive asymmetries and the open charm measurement, LSS: global analysis of inclusive and semi-inclusive asymmetries [13], DSSV: global analysis discussed below [6].

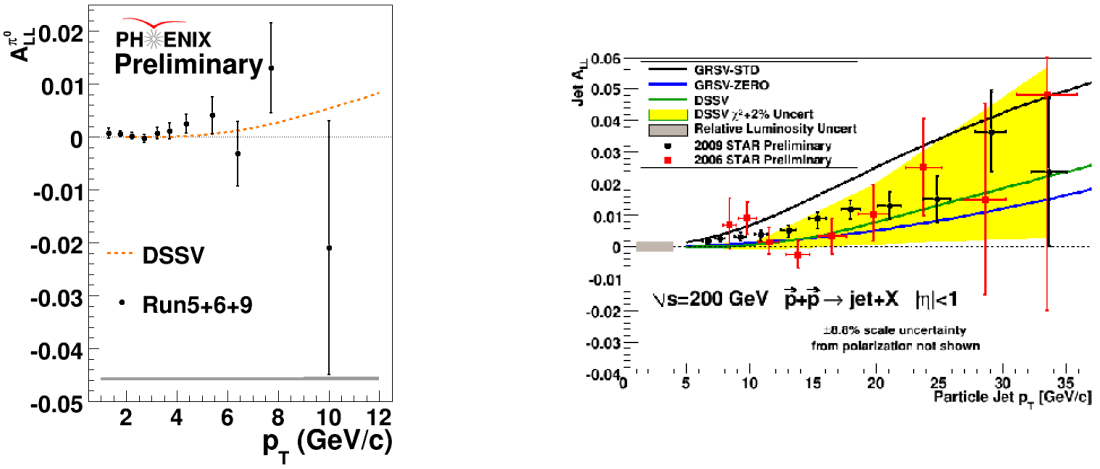

Figure 8: Double spin asymmetries in pp scattering from π^0 production (PHENIX) and jet production (STAR).

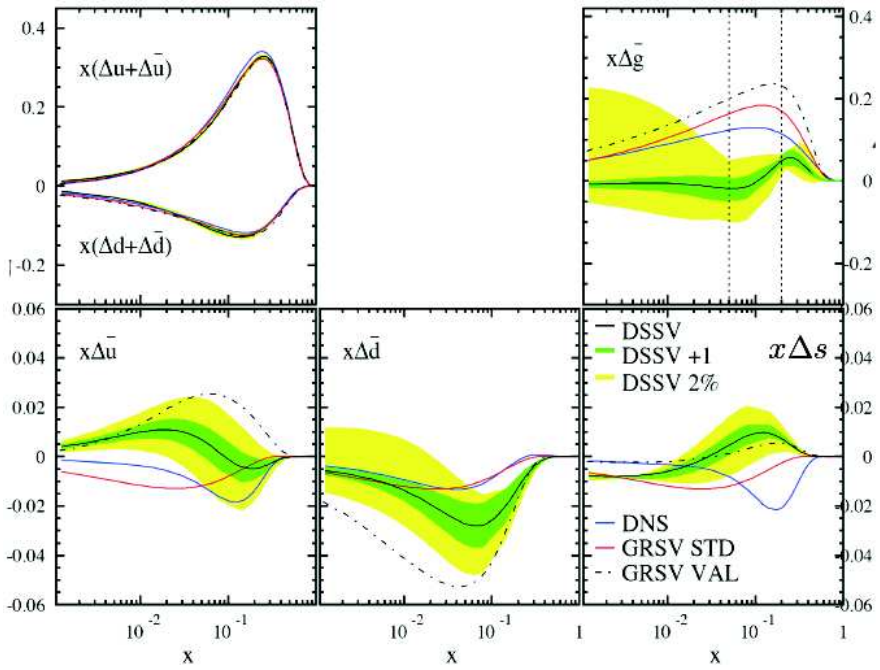

Figure 9: Results on helicity distributions from a global analysis [6].

largest influence on $\Delta g(x)$ comes from the pp data at RHIC. For the truncated first moment one finds

$$\int_{0.001}^{1} \Delta g(x) \mathrm{dx} = 0.013^{+0.702}_{-0.314}\,.$$

Note that the direct measurements from deep inelastic scattering are not yet included in this global analysis because for some channels a NLO QCD description is not yet available. Their inclusion will in the near future further constrain $\Delta g(x)$.

5 Future experimental programs

Table 2 gives an overview over some important parameter of past, present and future experiments in polarized deep inelastic scattering. In the near future experiments at JLAB, CERN, and BNL will continue to take data. Recently a new COMPASS proposal was accepted to study so called Generalized Parton Distributions in Deep Inelastic Virtual Compton Scattering (DVCS) and Hard Exclusive Meson Production (HEMP) as well as Transverse Momentum Dependent distributions (TMDs) in Drell-Yan processes [15, 16]. Similar programs are foreseen at JLAB and BNL.

Table 2 lists also projects for the far future. The electron ion collider (EIC) projects in the US are discussed in the contribution of J. Lee [17]. The project discussed in Europe at GSI, a

Table 2: Parameters of experiments to study deep inelastic scattering.

Experiment	JLab (12 GeV)	HERMES @DESY	ENC @FAIR/GSI	COMPASS @CERN	EIC @BNL/JLab
s/GeV^2	23	50	180	300	10000
$x_{bj,min} = \frac{1\mathrm{GeV}^2}{ys}$ for $y = 0.9$ and $Q^2 > 1\mathrm{GeV}^2$	$5 \cdot 10^{-2}$	$2 \cdot 10^{-2}$	$6 \cdot 10^{-3}$	$4 \cdot 10^{-3}$	10^{-4}
$\mathcal{L}/(1/\mathrm{cm}^2/\mathrm{s})$	$\approx 10^{38}$	$\approx 10^{32}$	$\approx 10^{32-33}$	$\approx 10^{32}$	$\approx 10^{33-34}$
$(P_T P_B f)^2$	0.026	0.16	0.41	0.026	0.24

3 GeV electron beam colliding with a 15 GeV proton beam has a center of mass energy and a luminosity comparable to the one of the running COMPASS experiment. The last line of the table gives the product squared of target, beam polarization and the target dilution factor. This quantity is of particular interest for double polarization experiments. Multiplied with the luminosity it gives an effective luminosity which is proportional to the figure of merit (= inverse squared of the statistical error) of the measured asymmetry. In this quantity one would gain a factor $0.41/0.026 \approx 16$. For the collider a polarization of 80% for both beams is assumed. In addition to this factor a large gain in hadron reconstruction is expected. In the case of a collider one does not suffer from hadron interactions in a solid state target. Such a collider, even at center of mass energies of already running experiments, would thus offer great opportunities for studies of the spin structure of the nucleon.

6 Summary & Outlook

It is well established since several years that the helicity contribution of quarks to the nucleon spin is only about $\Delta\Sigma = 25\%$ in contrast to a value of about 60% expected in relativistic quark models.

New data, mainly from semi-inclusive double spin asymmetries from the COMPASS experiment allowed to determine the contributions of the different quark flavors as a function of the Bjorken variable x to $\Delta\Sigma$. More data will decide whether the difference in the contribution of the light sea quarks $\Delta\overline{u}$ and $\Delta\overline{d}$ is only a statistical deviation. The RHIC experiment published first data on single spin asymmetries giving a direct access to the helicity distributions.

Concerning the gluon helicity distribution, the results indicate that the gluon distribution is small, but it should be kept in mind the error on the first moment is still on the order of 1/2, i.e. the gluon could still account for 100% of the nucleon spin.

New experimental programs at JLAB, CERN and BNL will continue in the near future measurements of the nucleon structure, where the interest will be enlarged to measurements of Generalized Parton Distributions (GPDs) and Transverse Momentum Dependent distributions (TMDs) giving also access to orbital angular momentum contributions. In the far future new facilities, like a polarized electron nucleon collider would offer great potential to study the spin structure of the nucleon at a much deeper level.

References

[1] E. Leader, Phys. Rev. D **83** (2011) 096012, [arXiv:1101.5956 [hep-ph]]

[2] S. Bass, The spin structure of the proton, World Scientific, 2008

[3] M. Anselmino, these proceedings

[4] R. D. Carlitz, J. C. Collins and A. H. Mueller, Phys. Lett. B **214** (1988) 229

[5] M. G. Alekseev *et al.* [COMPASS Collaboration], Phys. Lett. **B690** (2010) 466-472, [arXiv:1001.4654 [hep-ex]]

[6] D. de Florian, R. Sassot, M. Stratmann and W. Vogelsang, Phys. Rev. D **80** (2009) 034030

[7] E. Aschenauer, these proceedings

[8] J. D. Bratt *et al.* [LHPC Collaboration], Phys. Rev. D **82** (2010) 094502, [arXiv:1001.3620 [hep-lat]]

[9] N. Makke, these proceedings

[10] M. G. Alekseev *et al.* [COMPASS Collaboration], Phys. Lett. B **693** (2010) 227 [arXiv:1007.4061 [hep-ex]]

[11] J. S. Haggerty [PHENIX Collaboration], PoS **ICHEP2010** (2010) 149

[12] J. Balewski, APS meeting April 2010

[13] E. Leader, A. V. Sidorov, D. B. Stamenov, [arXiv:1012.5033 [hep-ph]]

[14] M. Stratmann, DIS 2010, Newport News, USA

[15] E.-M. Kabuß, these proceedings

[16] COMPASS II proposal
`http://wwwcompass.cern.ch/compass/proposal/compass-II_proposal/compass-II_proposal.pdf`

[17] J. Lee, these proceedings